Institute of Space and Aeronautical Science, University of Tokyo
Report No. 478, March 1972

Spherical Source Flow Expansion of Single Monatomic Gases into Vacuum*

By

Takeo SOGA**

Summary: The source flow expansion of single monatomic gases into a vacuum is studied on the basis of the B-G-K kinetic equation. The analysis is made by means of a numerical method proposed, in combining the discrete ordinate method. The actual calculations are carried out covering a spatial region from the isentropic upstream to the far downstream over a wide range of the Knudsen numbers, for both hard sphere and Maxwell molecules. It is found that in the far downstream the velocity distribution function is of asymmetric with respect to the radial velocity. The results for the macroscopic quantities are compared with the results of previous treatments, and found to be in a reasonable agreement with the numerical experiment by means of the Monte-Carlo method.

1. INTRODUCTION

In the free jet expansion into a vacuum, the flow is collision-dominated or isentropic in the vicinity of the orifice, while it becomes free molecular or collisionless in the far downstream from the orifice. Such phenomena appear in the exhaust from vehicles such as artificial satellites or rockets at high altitudes. Since the free jet expansion is rather complicated for the analysis, the expansion of gases from a point source into a vacuum has often been treated in order to clarify characteristic features associated with the phenomena. In fact, as pointed out by Sherman [*1*], the spherical source flow model may be quite a good representation of events along a jet center line. Quite apart from any applications these problems will contain a very important feature of the transition from continuum to free molecular flow in the absence of boundaries.

The problem concerned should be dealt with within the framework of kinetic theory. To the author's knowledge, it was done first by Brook and Oman [*2*] based on the B-G-K kinetic equation. Unfortunately, however, some of significant terms in the equation were ignored, so that the results are unlikely to be more than a qualitative estimate. After this work the moment-method analyses were performed based on the B-G-K kinetic equation by Edwards and Cheng [*3*] mainly

* This work is a part of the Doctor Thesis accomplished while the author was a postgraduate student in the Institute of Space and Aeronautical Science, University of Tokyo.

** Present address, Department of Aeronautics, Nagoya University, Nagoya.

focusing their attention to a far downstream region, and by Hamel and Willis [4] based on the Boltzman equation by matching the near-field solution with the far-downstream solution obtained with the hypersonic approximation. Recently an analysis similar to that by Hamel and Willis [4] was made by Chen [5] by preserving more higher moments. The results were found different appreciably from those of Hamel and Willis [4]. The moment method in general involves some uncertainty due to the arbitrariness in the truncation of higher order moments.

Although, in the present paper, we still retain the B-G-K kinetic model, we aim to obtain a more straightforward solution for the kinetic equation with far fewer approximations than the previous treatments. The solution is obtained by means of a numerical method proposed here, in combining the discrete-ordinate method. The actual calculations are carried out covering a spatial region from the isentropic upstream to the sufficiently far downstream over a wide range of the Knudsen number, for both hard sphere and Maxwell molecules.

2. Formulation of the Problem

The problem that we pose is illustrated in Fig. 1; we have a sphere of radius r_* from which gas is streaming with the velocity equal to the local speed of sound. The gas is allowed to expand radially, so that as $r\to\infty$ the density of gas will approach zero; we will be specifically interested in those conditions, for which source flow realises a supersonic expansion in the range $r>r^*$. The problem then is to predict the density, velocity, and temperature of the gas outward from the starting point of calculation ($r=r_1$) for the various source conditions.

To investigate this problem we use as our point of departure a numerical method; that is, discrete ordinate method. This method will allow us to analyse the problem without hypersonic approximation. We are specifically interested in two points; one is the breakdown of the isentropic expansion, and the other is the behavior of the expanding flow far downstream from the sonic radius. So we will start the calculation from the radius r_1 where the local Mach number of the

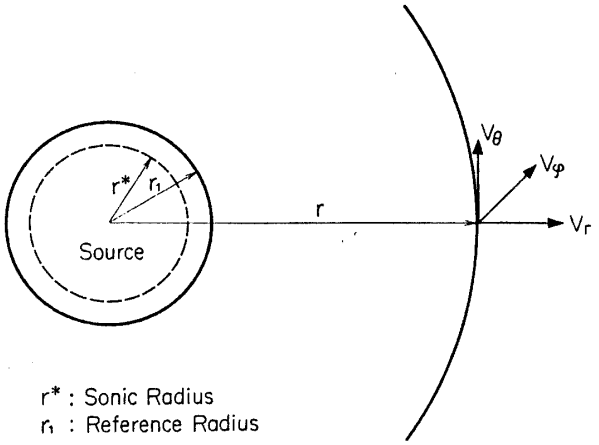

Fig. 1. Source flow expansion.

expanding flow is~2, i.e., $r^*<r_1<2r^*$. The problem is one-dimensional in physical space in that the distribution function $f(r, \vec{V}, t)$ describing the state of the system depends on r. The Boltzmann equation with the B-G-K collision model is chosen as the basic equation. In view of the geometrial symmetry the expression for this equation becomes in spherical coordinates (r, θ, φ) as follows:

$$V_r\frac{\partial f}{\partial r}+\frac{V_\theta^2+V_\varphi^2}{r}\frac{\partial f}{\partial V_r}-\frac{V_rV_\theta}{r}\frac{\partial f}{\partial V_\theta}-\frac{V_rV_\varphi}{r}\frac{\partial f}{\partial V_\varphi}=\nu(F-f) \qquad (1)$$

where F is the Maxwellian distribution pertinent to the number density, n, mean velocity U and temperature T, i.e.,

$$F=n(2\pi RT)^{-3/2}\exp\left[-(2RT)^{-1}\{(V_r-U)^2+V_\theta^2+V_\varphi^2\}\right] \qquad (2)$$

with the gas constant R. The collision frequency ν is given for gases obeying viscosity-temperature relation $\mu\propto T^s$ where the exponent s depends on the intermolecular force law, by $\nu=nkT/\mu$, where k is the Boltzmann constant.

Defining the radial and perpendicular temperatures, respectively, by

$$T_r=(nR)^{-1}\int_{-\infty}^{\infty}(V_r-U)^2f d\vec{V}, \qquad T_p=(2nR)^{-1}\int_{-\infty}^{\infty}(V_\theta^2+V_\varphi^2)f d\vec{V} \qquad (3)$$

where $\vec{V}$ is the velocity vector, we have

$$T=(T_r+2T_p)/3$$

Let us introduce the following dimensionless variables referred to the quantities at the radius $r=r_1$,

$$\begin{aligned} &r'=r/r_1, && n'=n/n_1, && U'=U/U_1,\\ &V_r'=V_r/V_1, && V_\theta'=V_\theta/V_1, && V_\varphi'=V_\varphi/V_1,\\ &T'=T/T_1, && T_r'=T_r/T_1, && T_p'=T_p/T_1,\\ &f'=(V_1^3/n_1)f, && F'=(V_1^3/n_1)f, && \nu'=\nu/\nu_1, \end{aligned}$$

where the subscript 1 denotes quantities at $r=r_1$ and $V_1=(2RT_1)^{1/2}$. Then the basic equation (1) and the associated macroscopic moments are rewritten in terms of the dimensionless variables. That is, Eq. (1) becomes

$$V_r'\frac{\partial f'}{\partial r'}+\frac{V_\theta'^2+V_\varphi'^2}{r'}\frac{\partial f'}{\partial V_r'}-\frac{V_r'V_\theta'}{\partial V_\theta'}\frac{\partial f'}{\partial V_\theta'}-\frac{V_r'V_\varphi'}{r'}\frac{\partial f'}{\partial V_\varphi'}=A\nu'(F'-f') \qquad (4)$$

Here F' is the nondimensionalised Maxwellian distribution

$$F'=n'(\pi T')^{-3/2}\cdot\exp\left[-\{(V_r'-S_1U')^2+V_\theta'^2+V_\varphi'^2\}/T'\right], \qquad (2')$$

where nondimensional parameters A and S_1 are as follows:

$$A=\frac{r_1\nu_1}{V_1}=\frac{r_1n_1kT_1}{V_1\mu_1}, \qquad S_1=\frac{U_1}{V_1} \qquad (5)$$

The macroscopic moments are obtained as follows:

$$n'=\int_{-\infty}^{\infty} f'd\vec{V}', \qquad U'=(n'S_1)^{-1}\int_{-\infty}^{\infty} V_r' f'd\vec{V}$$

$$T_r'=2(n')^{-1}\int_{-\infty}^{\infty}(V_r'-S_1U')^2 f'd\vec{V}', \qquad T_p'=n'^{-1}\int_{-\infty}^{\infty}(V_\theta'^2+V_\varphi'^2)f'd\vec{V}', \tag{6}$$

$$T'=(T_r'+2T_p')/3$$

The parameter A can be related to the Knudsen number $\mathbf{Kn}_1=L_1/r_1$ where L_1 is the mean free path at the reference radius. If the mean free path is given by

$$L_1=\frac{16}{5}\frac{\mu_1}{mn_1(2\pi RT_1)^{1/2}},$$

where m is the molecular mass, we have

$$A=(\pi)^{1/2}/2\mathbf{Kn}_1 \tag{7}$$

The parameters A and S_1 are not independent for the case when the expansion is isentropic from the sonic radius up to the reference radius $r=r_1$. For this sace a pair of parameters A and S_1 is related to the source Knudsen number **Kn** which is defined as $\mathbf{Kn}=L_0/D$, where L_0 is the mean free path at the stagnation and D the diameter of the orifice from which an equivalent free jet expansion blows out.

The primes denoting dimensionless variables may be omitted without any confusion, unless the specific note is provided. It is usuful to introduce two functions of r and V_r:

$$g(r, V_r)=r^2\int\int_{-\infty}^{\infty} f dV_\theta dV_\varphi, \qquad h(r, V_r)=r^4\int\int_{-\infty}^{\infty}(V_\theta^2+V_\varphi^2)f dV_\theta dV_\varphi \tag{8}$$

These functions [6] were first applied by Chu [7] in analyzing the unsteady plane shock problem, and afterwards by other investigators [3], [8]–[11] in analyzing various rarefied gas dynamic problems. By integrating Eq. (4) over (V_θ, V_φ), using the weighting functions r^2 and $r^4(V_\theta^2+V_\varphi^2)$, we obtain

$$V_r\frac{\partial g}{\partial r}+\frac{1}{r^3}\frac{\partial h}{\partial V_r}=A\nu(G-g) \tag{9}$$

$$V_r\frac{\partial h}{\partial r}+\tilde{h}=A\nu(H-h) \tag{10}$$

Here G and H are, respectively, the equilibrium values of g and h:

$$G=n(\pi T)^{-1/2}\exp\left[-(V_r-S_1U)^2/T\right], \qquad H=G\cdot T \tag{11}$$

and for abbreviation

$$\tilde{h}=\frac{\partial}{\partial V_r}\left[r^3\int\int_{-\infty}^{\infty}(V_\theta^2+V_\theta^2)^2 f dV_\theta dV_\varphi\right] \tag{12}$$

It should be noted that Eqs. (9) and (10) can be reduced to quite the same as those derived by Edwards and Cheng [3]. The macroscopic moments are written in terms of g and h as follows:

$$n=\int_{-\infty}^{\infty} g dV_r/r^2, \qquad U=\int_{-\infty}^{\infty} V_r g dV_r/nS_1r^2,$$

$$T_r=2\left(\int_{-\infty}^{\infty} V_r^2 g dV_r/r^2-nS_1^2U^2\right)\Big/n, \qquad T_p=\int_{-\infty}^{\infty} h dV_r/nr^4, \tag{13}$$

$$T=(T_r+2T_p)/3$$

The set of equations (9) and (10) contains the term $\tilde{h}$ still depending on the distribution f. To close a set of equations for g and h, therefore we shall make an additional assumption for the term $\tilde{h}$. The integral in Eq. (12) can formally be written as

$$\int\int_{-\infty}^{\infty}(V_\theta^2+V_\varphi^2)^2 f dV_\theta dV_\varphi=\beta\int\int_{-\infty}^{\infty}(V_\theta^2+V_\varphi^2) f dV_\theta dV_\varphi,$$

where β is the weighting function of r and V_r. In general, the β cannot be determined. If, however, the distribution function were of the ellipsoidal type

$$f=\frac{n}{(\pi T_r)^{1/2}(2\pi T_p)}\exp\left[-\frac{(V_r-S_1U)^2}{T_r}-\frac{V_\theta^2+V_\varphi^2}{T_p}\right]$$

then

$$\beta=2T_p.$$

Of course, this is also varid for the equilibrium distribution, in which $T=T_r=T_p$. We thus assume that the $\tilde{h}$ of Eq. (12) takes the form

$$\tilde{h}=\frac{2T_p}{r}\frac{\partial h}{\partial V_r} \tag{14}$$

Then, in Eq. (10) the ratio of the term $\tilde{h}$ to the first term takes the order

$$\tilde{h}/(V_r\partial h/\partial r)\sim T_p/V_r^2$$

Estimating that, as will be seen from the results, the perpendicular temperature T_p may be close to the equilibrium value, the above relation becomes

$$\tilde{h}/(V_r\partial h/\partial r)\sim(M_1/M)^2$$

where $M=U'(RT')^{-1/2}$ is the Mach number (prime denotes dimensional variables). We can see that the term $\tilde{h}$ has no appreciable contribution over a far downstream region of high Mach number. Since the approximation Eq. (14) for the term $\tilde{h}$ is valid in the equilibrium region near the sonic radius, it may cause no significant error for the solution as a whole. It should be noted that a set of equations (9) and (10) with this approximation for $\tilde{h}$ still leads to the rigorous macroscopic

transfer equations of mass, momentum, and energy.

Our considerations are confined to the cases when the flow is in equilibrium within a moderate distance downstream from the sonic radius. We now choose a certain radius $r=r_1$ within that region, as the reference. On the other hand, the density vanishes at infinite downstream. The boundary conditions are thus specified as follows:

$$\begin{aligned} r=1, \qquad & g_1=\pi^{-1/2}\exp\left[-(V_r-S_1)^2\right], \\ & h_1=\pi^{-1/2}\exp\left[-(V_r-S_1)^2\right]. \end{aligned} \tag{15}$$

3. Computative Procedure

Following the discrete ordinate method which has already been developed for the analyses of several rarefied flow problem (for example, see Reference 10), the velocity space V_r is represented by finite discrete points, say V_n ($n=1, 2, 3, \cdots, m$). The application of the method reduces the set of governing integro-differential equations, Eqs. (9) and (10) to a set of ordinary differential equations. That is, the resulting differential equations are

$$V_n\frac{dg_n}{dr}+\frac{1}{r^3}\left(\frac{\partial h}{\partial V_r}\right)_n=A\nu(G_n-g_n) \tag{16}$$

$$V_n\frac{dh_n}{dr}+\frac{2T_p}{r}\left(\frac{\partial h}{\partial V_r}\right)_n=A\nu(H_n-h_n) \tag{17}$$

where

$$G_n=n(\pi T)^{-1/2}\exp\left[-(V_n-S_1U)^2/T\right], \qquad H_n=G_nT \tag{18}$$

and

$$\nu=nT^{(1-s)} \tag{19}$$

Here g_n, h_n, G_n, and H_n represent g, h, G, and H evaluated at the discrete velocity points V_n ($n=1, 2, 3, \cdots, m$), respectively.

The boundary conditions become

$$r=1, \quad g_{1_n}=\pi^{-1/2}\exp\left[-(V_n-S_1)^2, \quad h_{1_n}=\pi^{-1/2}\exp\left[-(V_n-S_1)^2\right]\right. \tag{20}$$

Thus, the problem reduces to solving Eqs. (16) and (17) subject to the conditions (20). This yields $2m$ equations with $2m$ discrete unkowns g_n and h_n.

In the discrete ordinate scheme, the velocity V_n acts only as parametric variables. Therefore the equations (16) and (17), respectively, for g_n and h_n can be solved by applying an ordinary difference scheme to physical space r. The reduced distributions g_n and h_n conveniently divided into a two-sided one; $g_n^{\pm}$ for $V_n\gtrless 0$ and $h_n^{\pm}$ for $V_n\gtrless 0$. The difference form of Eq. (16) for g_n^{+} becomes

$$V_n \frac{g_n^+(r)-g_n^+(r-\Delta r)}{\Delta r}+\frac{1}{r^3}\left(\frac{\partial h^+}{\partial V_r}\right)_n=A\nu(r)(G_n^+(r)-g_n^+(r)) \tag{21}$$

where Δr is the radial increment. Rearranging Eq. (21), we obtain

$$g_n^+(r)=\frac{(V_n/\Delta r)g_n^+(r-\Delta r)+A\nu(r)G_n^+(r)-r^{-3}(\partial h^+/\partial V_r)_n(r)}{V_n/\Delta r+A\nu(r)} \tag{22}$$

In quite a similar way we obtain the difference form for h_n^+ as follows:

$$h_n^+(r)=\frac{(V_n/\Delta r)h_n^+(r-\Delta r)+A\nu(r)G_n^+(r)-(2T_p/r)(\partial h^+/\partial V_r)_n(r)}{V_n/\Delta r+A\nu(r)} \tag{23}$$

Remembering the assumption that there exists an equilibrium region near the sonic radius, we may choose the reference radius $r=r_1$ where the flow is moderately supersonic. In the actual calculation, the reference radius r_1 was chosen such that the flow Mach number there is ~ 2.0. For such a case the contribution of g_n^- (for $V_n<0$) is much smaller compared with that of g_n^+ even in the vicinity of the reference radius. In the far downstream region, evidently the contribution of g_n^- become negligibly small. In view of the aforementioned facts, both g_n^- and h_n^- were not taken into account in the present paper.

A. *Method of Evaluation of the Derivative $\partial h/\partial V_r$*

The reduced distribution h can be expressed in the form of

$$h=\exp\Theta(V_r), \tag{24}$$

in which $\Theta(V_r)$ is determined to fit. Consistent with the facts that function $\Theta(V_r)$ takes a quadratic for the case of the equilibrium distribution, we approximate the function $\Theta(V_r)$ around the point $V_r=V_n$ by quadratic form as

$$\Theta(V_r)=a_0+a_1V_r+a_2V_r^2,$$

in which the coefficients a are determined so as to satisfy Eq. (24) at the three neighboring points, say V_{n-1}, V_n, V_{n+1}. Then, the derivative $(\partial h/\partial V_r)_n$ at the point $V_r=V_n$ can be evaluated from

$$\partial h/\partial V_r=(a_1+2a_2V_r)h$$

The method proposed above was applied to the bimodal distribution of an analytic form, and its applicability was assured from comparison of the calculated values with the exact values.

B. *Selection of Discrete Velocity Points*

In a source expansion flow the profile of distribution function rapidly becomes steeper with decreasing temperature in proceeding downstream. Accordingly one fixed set of discrete velocity points is not efficient to fit all the velocity distribution functions throughout the whole spatial region, because a great number of velocity points is needed to do it.

As shown schematically in Fig. 2, the spatial region may conveniently be divided into several subdomains designated as Region 1, Region,... Suppose that in Region k the radial temperature and mean velocity are represented by the averaged values $\bar{T}^k$ and $\bar{S}^k$, where the superscript k refers to the quantities in Region k. As can be seen from Fig. 2, the $\bar{T}^k$ and $\bar{S}^k$ provide the measure, respectively, for the spread and ordinate of the reduced velocity distribution function g. For Region k, therefore the following set of discrete velocity points will be employed as an appropriate choice,

$$V_n^k=(\bar{T}^k)^{1/2}\cdot C_n+\bar{S}^k \qquad (n=1,2,3,\cdots,m) \tag{25}$$

Here C_n is the discrete ordinate of thermal velocity, being chosen so as to fit the

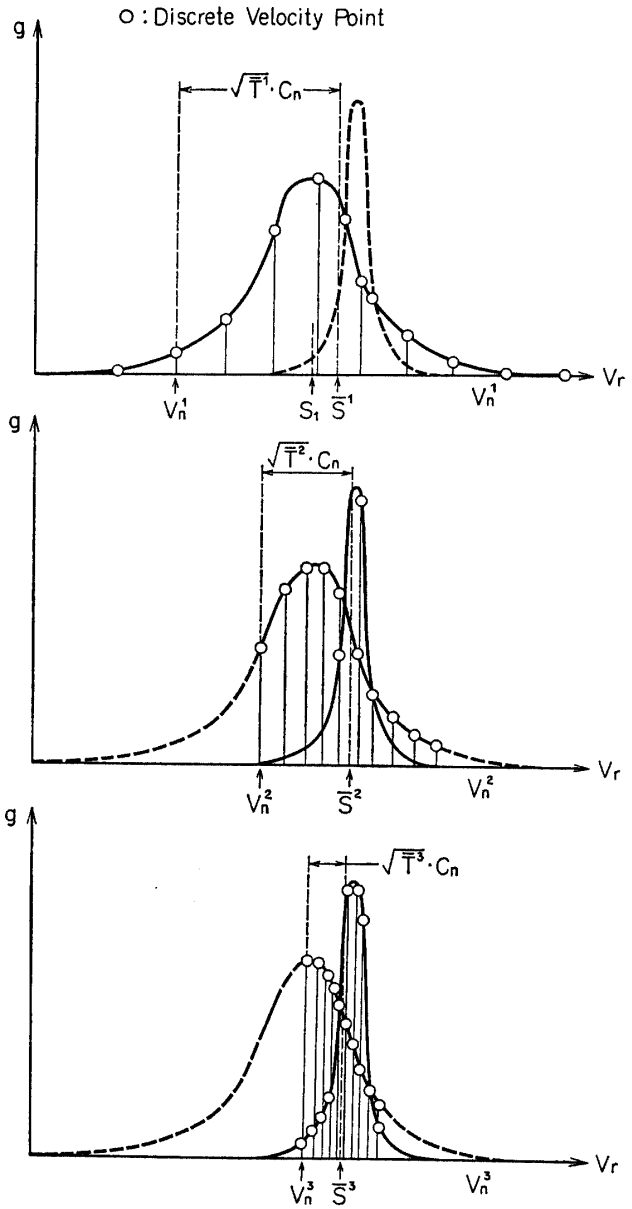

FIG. 2. Sets of discrete velocity points.

velocity distribution at the reference radius $r=r_1$, and m is the number of velocity points. In the present calculation the 10 velocity points are used, so that $m=10$. In proceeding the step-by-step calculation in Region k, the integration for the evaluation of macroscopic moments is carried out based on the set k of velocity points, by means of the ten-point Gauss-Hermite quadrature. The temperature thus evaluated decreases from step to step. The calculation for Region $k+1$ is initiated when one reaches the step where the temperature becomes equal to or less than $(\bar{T}^k \cdot \bar{T}^{k+1})^{1/2}$. In the actual calculation, the temperature T_r ranged 1 up to $1.0 \cdot 10^{-3}$ and three sets of discrete velocity points were applied according to the procedure mentioned above.

C. *Iterative Procedure*

Following the difference scheme Eqs. (22) and (23), the evaluation of the reduced distributions g_n^+ and h_n^+ is advanced step by step, starting from the reference radius. At each step, however, a number of iterations are required to reach a solution. Suppose that we know all the values of quantities at the radius $r-\Delta r$. As the initial estimate of the quantities on the right hand side of Eqs. (22) and (23), their respective values at the previous step are employed, in which case the derivative $\partial h_n^+/\partial V_r$ can be evaluated for the known $h_n^+(r-\Delta r)$ by the method of Sec. 3A. Using thet zeroth interate g_n^+ and h_n^+ thus evaluated, the new macroscopic moments can be determined by applying the ten-point Gauss-Hermits quadrature to the integration of Eqs. (13). Then, all the terms on the right hand side of Eqs. (22) and (23) are reevaluated. Such a procedure is iterated until a satisfactory convergence has been assured for all velocity points; normally, three or four iterations were sufficient to fullfil, for both number density and mean velocity, the convergence criteria that the departure from the previous iterate must be less than 10^{-6} times their respective values. The accuracy of the calculation was estimated by examining the constancy of mass flux. The error in the step-by-step calculation accumulates as it proceeds downstream. The actual computation was stopped at the point, beyond which the value of mass flux indicates a departure more than 1% from that at the reference radius. This implies that the maximum error in mass flux is less than 1%. The spatial region, thus computed with the increment being $\Delta r=r/100$, was covered from $r/r^*=r_1/r^*$ to $r/r^*=10^4$, where r^* is the sonic radius.

4. Numerical Results

In the present section as well as in the figures, the symbols for dimensional quantities will be used. The HITACH 5020F digital computer was used for the calculation. The numerical analysis was carried out for both hard sphere and Maxwell molecules for various Knudsen numbers **Kn** ranged from about 3.0 to $1.0.10^{-5}$. The Knudsen number **Kn** is one most commonly used in reporting free-jet experiments, being defined as the ratio of stagnation mean free path to the orifice diameter D. Since the orifice diameter D is related to the sonic radius r^*,

we can deduce **Kn** to the **Kn*** ($=L_0/r^*$) as well as **Kn**$_1$ defined previously.

As mentioned before, the computation was started from the reference radius r_1 where the flow is assumed to be in equilibrium. There arises a question as to whether the solution depends on a choice of the reference radius r_1. If the equilibrium condition is valid at the reference radius, the solution should be uniquely determined over a whole downstream region from the referenec radius. This may be justified if the solution for the slight alternation of r_1 (for instance, for two radii corresponding to $M=2$ and 3) indicates no appreciable difference each other. Otherwise, the solution is unlikely to be realistic from a physical point of view. Although this will be discussed later in more detail, the assumption appears to be valid for cases of **Kn** $\lesssim 10^{-2}$.

A. *Behavior of density*

In Fig. 3 is shown profile of the density distributions for the various Knudsen number **Kn**. The detail comparison of the density n with its isentropic value n_E is made in Figs. 4 and 5, respectively, for the hard sphere and the Maxwell molecules. It can be seen from these figures that the density is greater than its isentropic values throughout the expansion, for the stagnation Knudsen number **Kn** $\gtrsim 1$, and also that the density nearly coincides with its isentropic values for the **Kn** less than 10^{-3}.

B. *Mean velocity and its terminal values*

In Figs. 6 and 7 is shown the mean velocity U, respectively, for the hard sphere

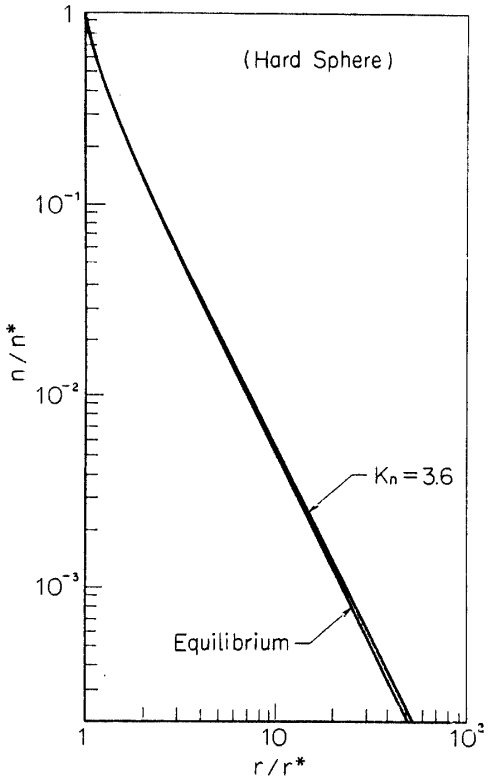

FIG. 3. Number density distribution.

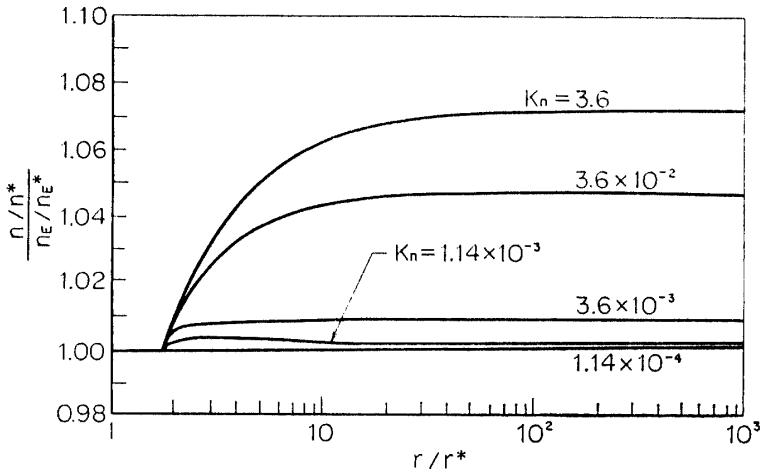

FIG. 4. Distributions of number density ratio (n/n_E) (for hard sphere molecules).

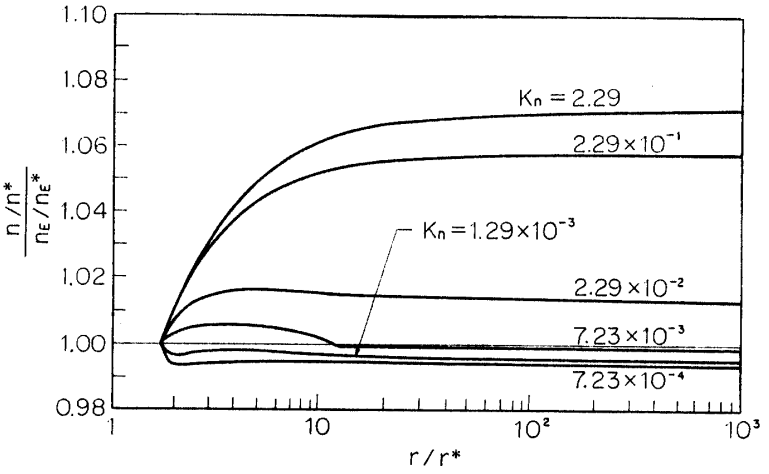

FIG. 5. Distributions of number density ratio (n/n_E) (for Maxwell molecules).

and for the Maxwell molecules. The velocity distribution along the radial line is much closer to that of the isentropic expansion for the Maxwell molecules than for the hard sphere. For both molecular models, the terminal mean velocity depends on the **Kn**. In Fig. 8 is plotted the terminal velocity against the source Knudsen number **Kn**. It follows that for the Maxwell molecules the kinetic energy amounts more than 99.9% of the total energy for the $\mathbf{Kn} \leq 10^{-3}$, while for the $\mathbf{Kn} > 10^{-3}$ an appreciable amount remains as the thermal energy. The similar trend can be seen for the case of the hard sphere, in which the critical value of **Kn** is $\sim 10^{-4}$. The fact mentioned above implies that the transfer from thermal energy to kinetic energy through the expansion is achieved by the collisions among gases particles.

C. *Temperature and its terminal values*

The ratio of the temperature T to the sonic temperature T^* is plotted against the radius r in Figs. 9 and 10, respectively, for the hard sphere and for the Max-

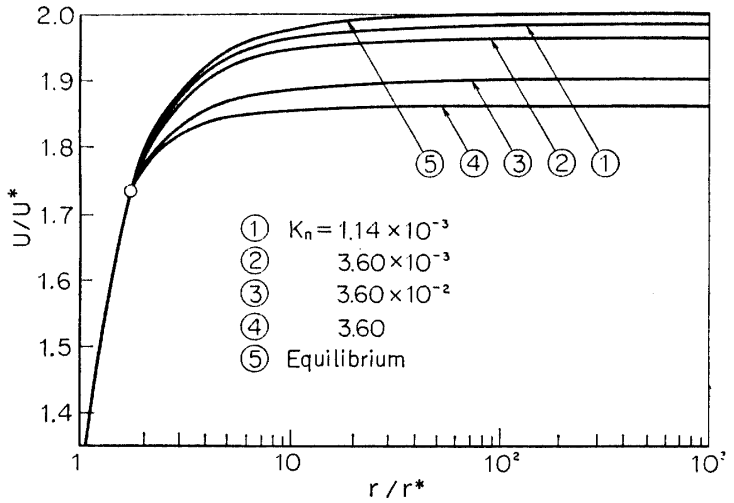

FIG. 6. Mean velocity distributions (for hard sphere molecules).

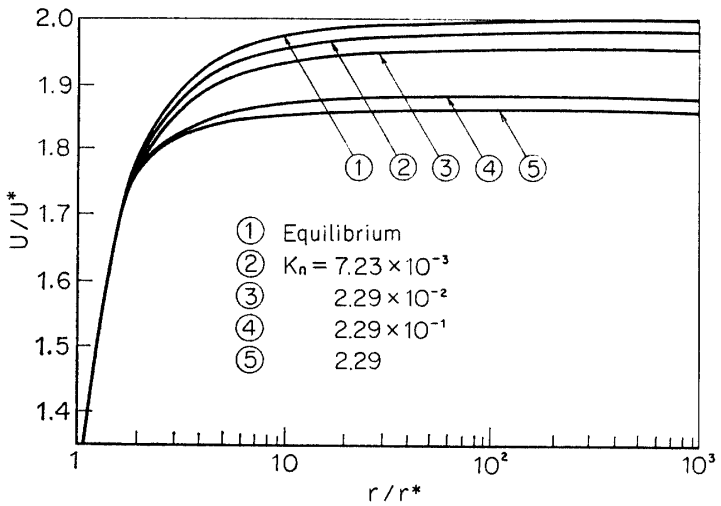

FIG. 7. Mean velocity distributions (for Maxwell molecules).

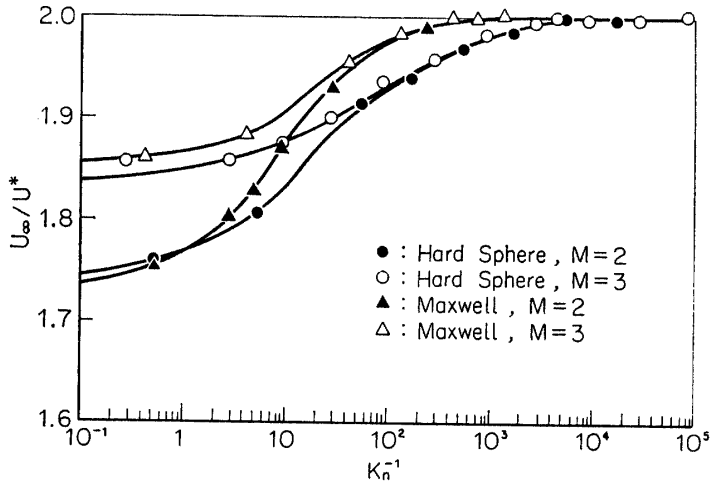

FIG. 8. Terminal mean velocity *vs* source Knudsen number **Kn**.

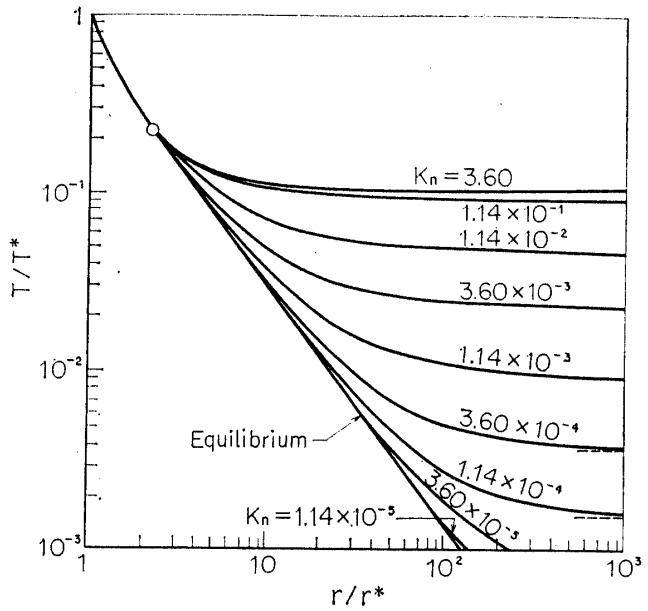

FIG. 9. Temperature distributions (for hard sphere molecules).

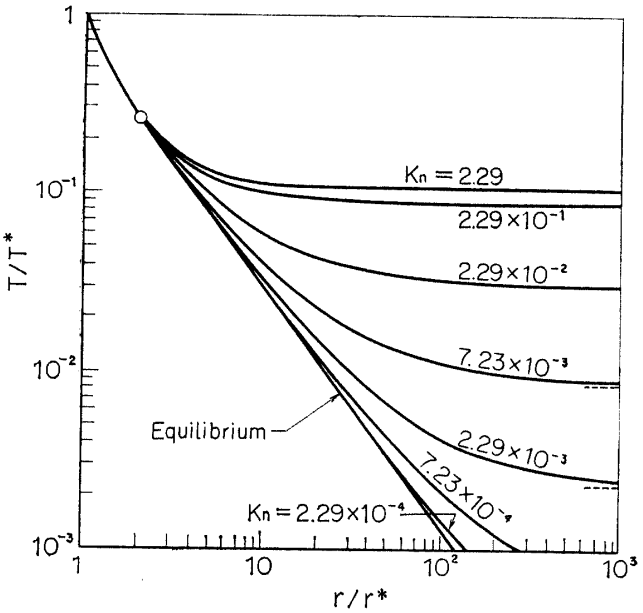

FIG. 10. Temperature distributions (for Maxwell molecules).

well molecules. For a fixed **Kn** the temperature distribution indicates a feature much closer to that of the isentropic expansion for the Maxwell molecules than for the hard sphere. In Figs. 11–14 are shown the distributions of the radial temperature T_r and perpendicular temperature T_p. The behavior of radial temperature T_r is similar to that of the temperature T and the "freezing" of the radial temperature begins to occur at more earlier stage in the expansion than for the "freezing" of the temperature. Except the case of the Knudsen number $\mathbf{Kn} > 10^{-2}$, the perpendicular temperature shows no appreciable departure from its isentropic

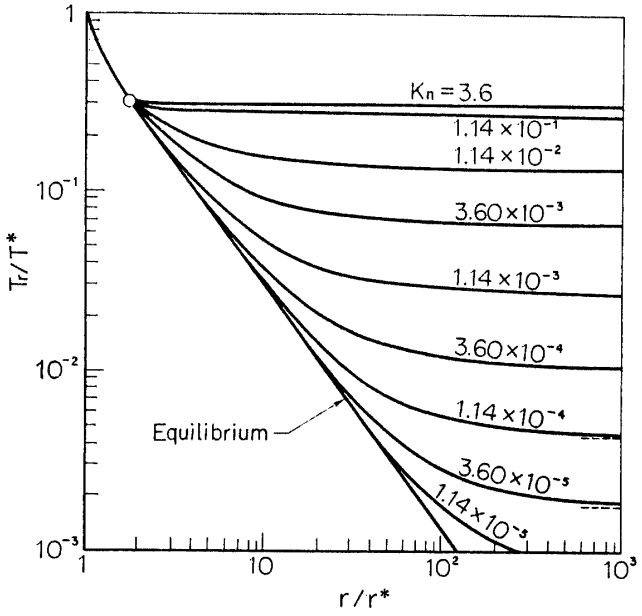

FIG. 11. Radial temperature distributions (for hard sphere molecules).

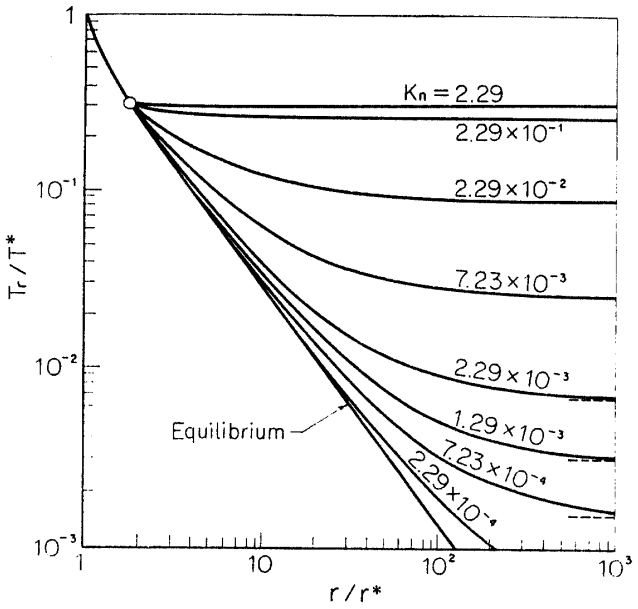

FIG. 12. Radial temperature distributions (for Maxwell molecules).

value over a wide region ($r \lesssim 10^2 r^*$). In proceeding a further downstream, the perpendicular temperature T_p begins to depart from the isentropic values, and asymptotically approaches $T_p = \text{const.}(r^*/r)$.

In Fig. 15 are plotted both terminal temperature T_∞ and terminal radial temperature $T_{r\infty}$ against the source Knudsen number **Kn**. These were evaluated from the solutions obtained for the two different values of the reference radius r_1; one is the radius of the flow Mach number $M=2.0$, and the other the radius

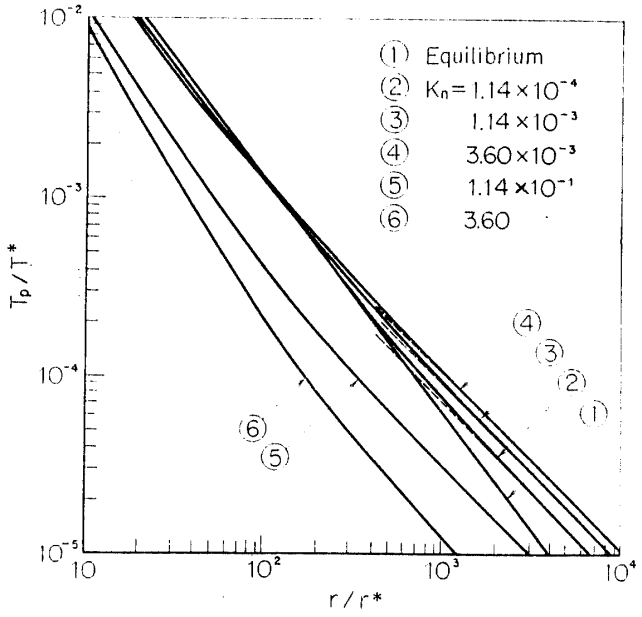

FIG. 13. Perpendicular temperature distributions (for hard sphere molecules): —asymptotic straight line $\sim r^{-1}$.

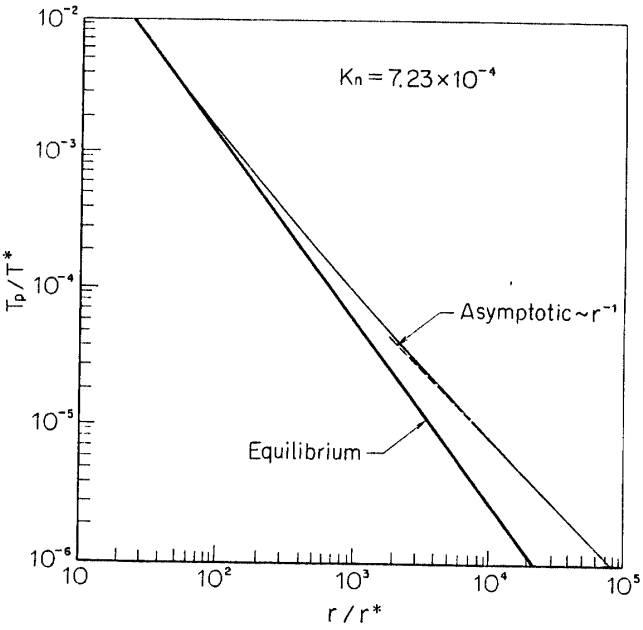

FIG. 14. Perpendicular temperature distribution (for hard spere molecules): —asymptotic straight line $\sim r^{-1}$.

of $M=3.0$. We can see from this figure that the temperatures T_∞ and $T_{r\infty}$ indicate an appreciable dependence on the reference radius, for either cases of hard sphere or Maxwell molecules, for $\mathbf{Kn}>10^{-2}$. As mentioned before, the present solution may be considered valid only when it does not depend on the choice of the reference radius. Therefore, we say the present results are of significance for the cases of $\mathbf{Kn}\lesssim 10^{-2}$.

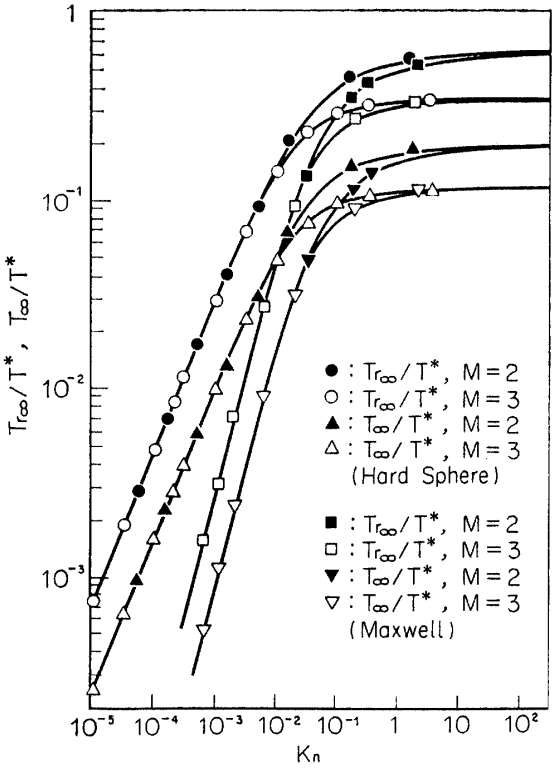

FIG. 15. Terminal temperature and Terminal radial temperature *vs* Source Knudsen number **Kn**.

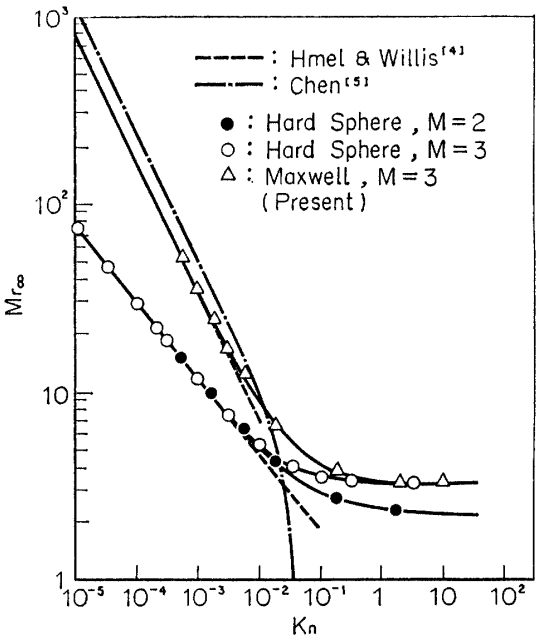

FIG. 16. Terminal Mach number *vs* Source Knudsen number **Kn**.

5. COMPARISON WITH PREVIOUS RESULTS AND DISCUSSION

In Fig. 16 is plotted the terminal Mach number vs source Knudsen number *Kn*. Hamel and Willis [*4*] found the formulae for the dependence of terminal Mach number on the Knudsen number from their analysis. The comparison with the formulae derived by the present results is made for the terminal Mach number $M_{r\infty}$ referred to radial temperature in the following,

	Present	Hamel and Willis[4]
for hard sphere	$M_{r\infty}=0.80\,\mathbf{Kn}^{-0.40}$,	$=0.77\,\mathbf{Kn}^{-0.40}$,
for Maxwell	$M_{r\infty}=0.42\,\mathbf{Kn}^{-0.67}$,	$=0.42\,\mathbf{Kn}^{-0.67}$,

where $M_{r\infty}=U_\infty/(RT_{r\infty})^{1/2}$ and is approximately equal to $M_\infty/(3)^{1/2}$.

We can see that the present results are in an excellent agreement with those by Hamel and Willis [*4*]. An analysis by the moment method similar to Hamel and Willis' was worked out by Chen [*5*] in taking into account more higher order moments. However, his results indicate somewhat appreciable deviation from the present results. Therefore, no better results are expected for the moment method by preserving more higher order moments.

As regards the radial temperature, in Fig. 17 is made comparison of the present results with the Muntz's experiment [*12*] using the electron beam fluorescence tech-

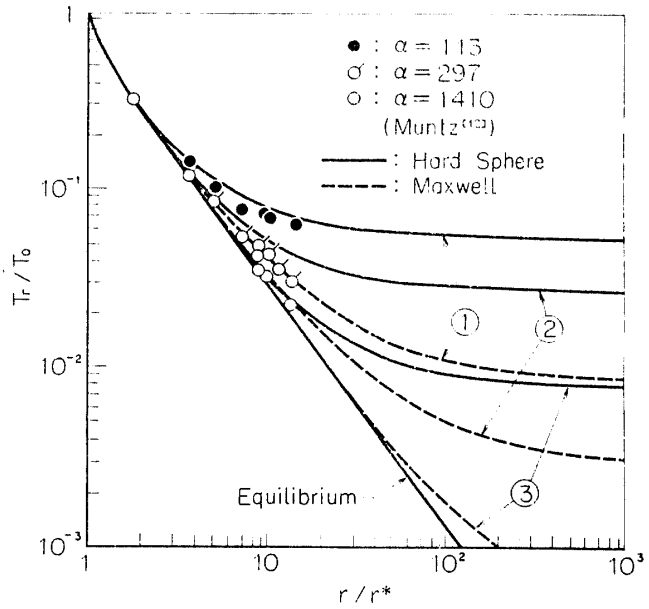

FIG. 17. Comparison with the results of Muntz[12]: ① $\alpha=113$, ② $\alpha=297$, ③ $\alpha=1410$.

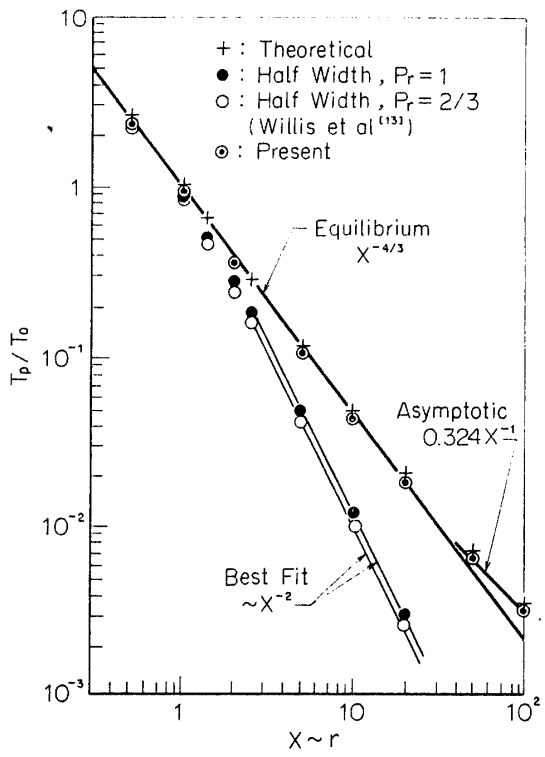

FIG. 18. Comparison with the results by Willis *et al*[13] (for hard sphere molecules).

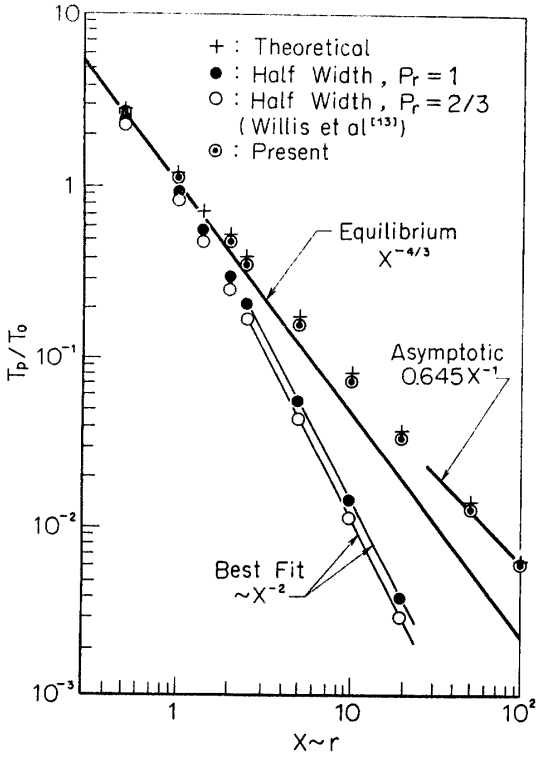

FIG. 19. Comparison with the results by Willis *et al*[13] (for Maxwell molecules).

nique. In this figure the parameter $\alpha=0.413\ Kn^{-1}$ introduced by Hamel and Willis [4] is used. The experimental data for argon lie between the solution obtained for the hard sphere and for the Maxwell molecules. In the analysis the molecular model affects the solution only through the value of s, the exponent contained in the viscosity-temperature relation. Bearing in mind the fact that $s=1.0$, 0.8, 0.5, respectively, for the Maxwell molecules, argon and hard sphere molecules, the agreement of the present results with the experiment appears to be quite reasonable.

Willis and Hame [13] found the profile of velocity distribution function by the method of characteristics based on the EDF (ellipsoidal distribution function) model equation for the hypersonic limite. As predicted by Scott [14] *et al.* the perpendicular temperature evaluated from the half width of the distribution function is found to be inversely proportional to the square of radius r. In Figs. 18 and 19 is made comparison of the present results with the Willis and Hamels' [13],

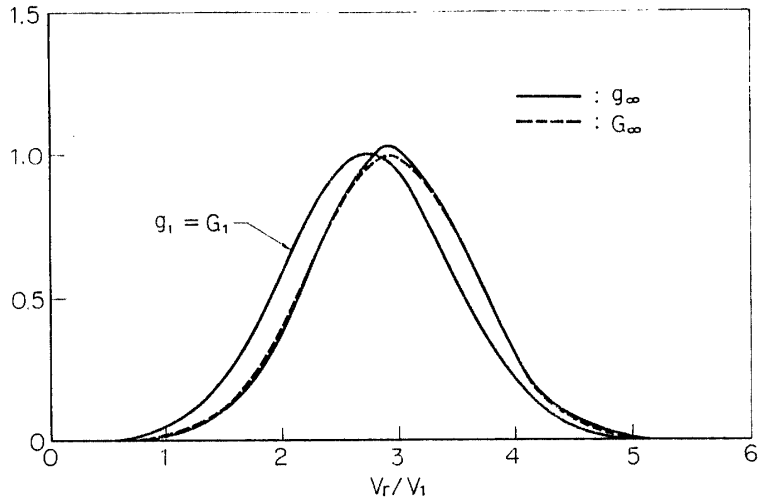

FIG. 20. Terminal velocity distribution function ($Kn\lesssim 1$).

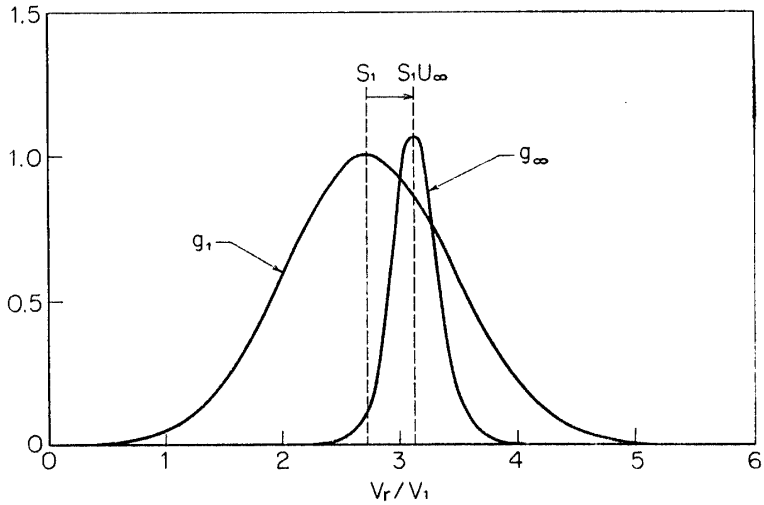

FIG. 21. Terminal velocity distribution ($Kn\ll 1$).

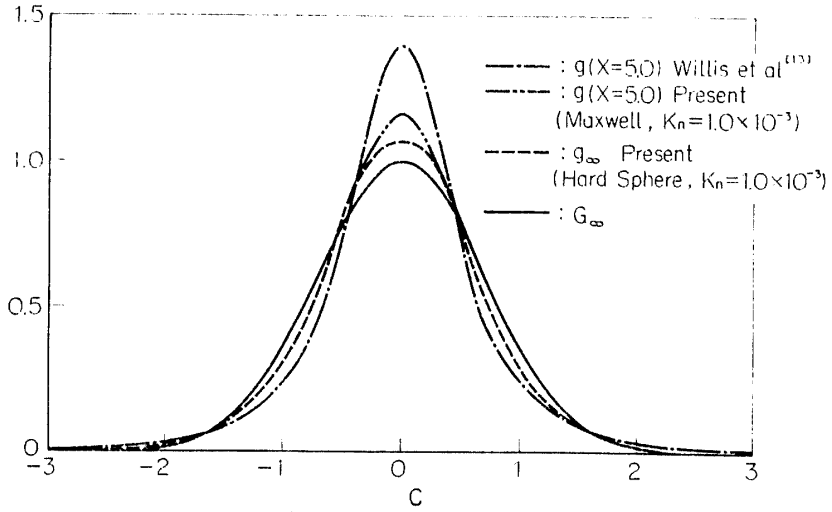

FIG. 22. Comparison with the results by Willis et al[13].

respectively, for the hard sphere and for the Maxwell molecules. In these figures the coordinate X is one non-dimensionalised by the radius on which $T_r - T_p = T_{\text{isen}}$. We can see the excellent agreement of the present results with the Willis and Hamels' [*13*]. In Figs. 20 and 21 is shown the profile of the velocity distribution function both for $r=r_1$ and $r\to\infty$, for the various source Knudsen numbers. For the source Knudsen numbers large, the terminal distribution function g_∞ shows only a slight deviation from the equilibrium G_∞ (see Fig. 20). By introducing

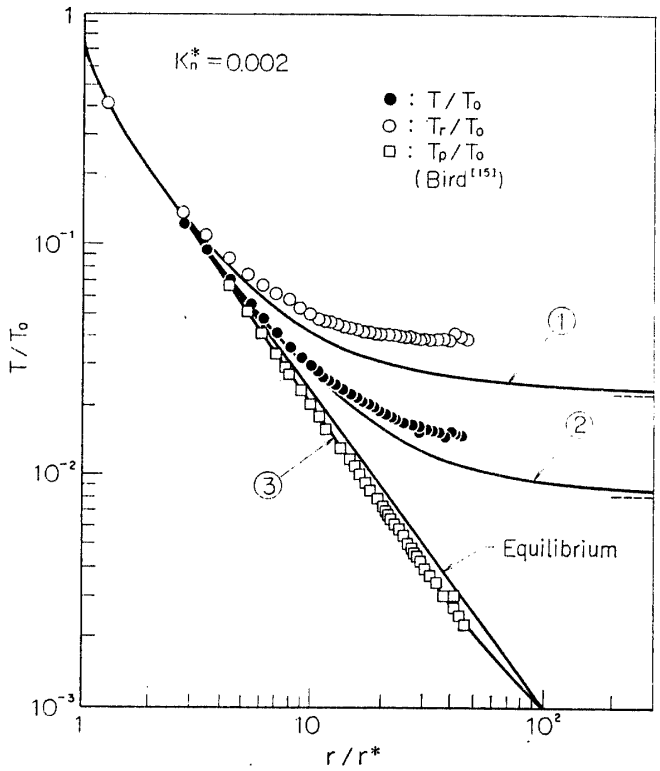

FIG. 23. Comparison with the results by Bird[15] (for hard sphere molecules): ①$=T_r/T_0$, ②$=T/T_0$, ③$=T_p/T_0$.

the ordinate C defined by $C=(V_r-U_\infty)/(T_{r\infty})^{1/2}$, the results are re-plotted in Fig. 22, in which the distribution functions obtained by Willis and Hamel [*13*] are also plotted. In contrast to the symmetric nature of the ellipsoidal distribution assumed in the Willis and Hamels [*13*] analysis, the distribution function obtained in the present analysis indicates an asymmetric nature. This implies that the present analysis may lead the results different from those by the Willis and Hamel' [*13*] analysis for the quantities pertinent to the higher moments (for example, heat fluxs).

Recently Bird [*15*] conducted a kind of numerical experiments for the source flow problem by means of the Monte-Carlo direct simulation method. In Figs. 23 and 24 is indicated comparison of the present results with those by Bird [*15*] for the cases of both hard sphere and Maxwell molecules. The Knudsen number **Kn*** is defined as $\mathbf{Kn}^*=L_0/r^*$, where L_0 is the mean free path for the stagnation condition. It can be seen from these figures that as a whole the present results show a better agreement with Bird's [*15*] results for the Maxwell molecules than for the hard sphere molecules. This is consistent with the fact that the B-G-K collision model is basically relevant to the Maxwell molecules. In Fig. 25 a similar comparison to the previous is made for the several Knudsen numbers. It can be seen that the agreement of the present results with Bird's [*15*] becomes much better for smaller Knudsen numbers. If the Bird's [*15*] results provide a representation of the exact Boltzman solution, the agreement of the present results gives a support

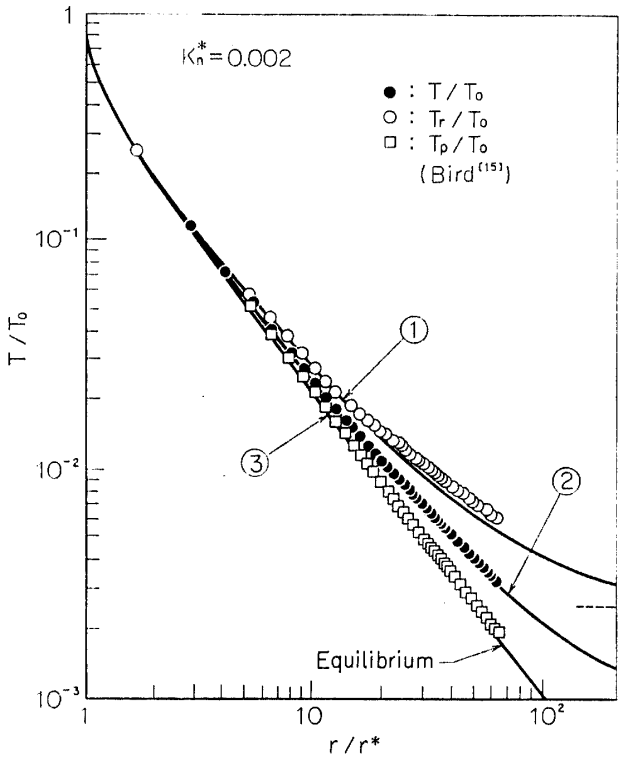

FIG. 24. Comparison with the results by Bird[15] (for Maxwell molecules): ①$=T_r/T_0$, ②$=T/T_0$, ③$=T_p/T_0$ ($\approx T_E$).

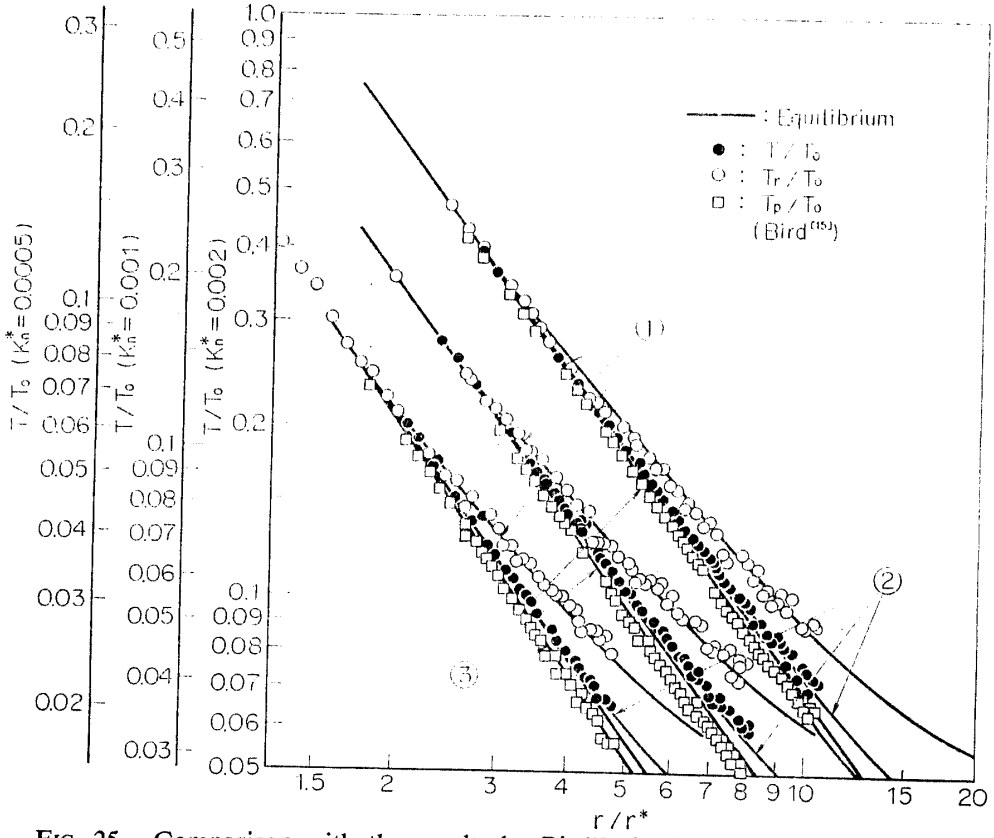

FIG. 25. Comparison with the results by Bird[15] (for hard sphere molecules): ①$=T_r/T_0$, ②$=T/T_0$, ③$=T_p/T_0$.

for the applicability of the B-G-K kinetic equation to the source flow expansion problem.

In conclusion the B-G-K kinetic equation has numerically been solved for the source flow expansion of monatomic gases into a vacuum, with far fewer approximations than the previous treatments. The results have been compared with the previous ones, and, particularly, they are found to be in a fairly good agreement with the numerical experiment of Bird. Finally it is hoped that the numerical method proposed here will allow us to treat the rarefied gas dynamic problem based on the kinetic equation subject to the cylindrical or spherical coordinates.

ACKNOWLEDGEMENT

The author wishes to express his sincere gratitude to Professor Hakuro Oguchi for his valuable discussion and constant support during the course of this investigation.

Department of Aerodynamics
Institute of Space and Aeronautical Science
University of Tokyo, Tokyo
January 15, 1972

REFERENCES

[1] H. Ashekenas and F. S. Sherman, "*Rarefied Gas Dynamics*" (Academic Press Inc., New York, 1966), Vol. II, p. 84.
[2] J. W. Brook and R. A. Oman, "*Rarefied Gas Dynamics*" (Academic Press Inc., New York, 1965), Vol. I, p. 125.
[3] R. H. Edwards and H. K. Cheng, AIAA. J. **4**, 558 (1966).
[4] B. B. Hamel and D. R. Willis, Phys. Fluids **9**, 829 (1966).
[5] T. Y. Chen, Phys. Fluids **13**, 317 (1970).
[6] Note that the functions g and h defined here are different from those in Ref. 3, respectively, by the multiplication factor r^2 and r^1.
[7] C. K. Chu, Phys. Fluids 8, 12 (1965).
[8] G. Bienkowski, "*Rarefied Gas Dynamics*" (Academic Press Inc., New York, 1965), Vol. I, p. 71.
[9] K. Abe and H. Oguchi, "*Rarefied Gas Dynamics*" (Academic Press Inc., New York, 1969), Vol. I, p. 425.
[10] A. B. Huang and D. P. Giddens, Phys. Fluids **10**, 232 (1967).
[11] A. A. Peracchio, AIAA. J. 8, 1665 (1970).
[12] E. P. Muntz, "*Rarefied Gas Dynamics*" (Academic Press Inc., New York, 1967), Vol. II, p. 1257.
[13] D. R. Willis, B. B. Hamel and J. T. Lin, College of Engineering, University of California, Berkley, Report No. as-70-8.
[14] J. E. Scott, Jr., and J. A. Phipps, "*Rarefied Gas Dynamics*" (Academic Press Inc., New York, 1967), Vol. II, p. 1317.
[15] G. A. Bird, AIAA. J. 8, 1998 (1970).